Transition mode PFC controller for flyback converters
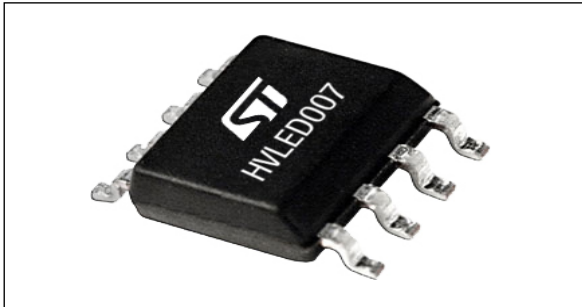
Features

- Transition-mode (quasi-resonant) control of flyback PFC pre-regulators
- Proprietary input current shaper for minimum THD of line current
- Control input for isolated feedback and optocoupler driving
- Output overvoltage protection
- Overload and short-circuit protection
- Low (≤ 60 µA) start-up current and low (≤ 4 ma) quiescent current
- Digital leading-edge blanking on current sense
- -600/+800 mA totem pole gate driver with UVLO pull-down and voltage clamp
- SO8 package

Applications

Flyback PFC converters for:

- AC-DC LED drivers for domestic, commercial and industrial lighting
- Street lighting
- EN61000-3-2 compliant SMPS

Description

The HVLED007 is a current-mode PFC controller specific for isolated high power factor, flyback

converters operated in transition mode (aka quasi-resonant operation). Targeting both indoor and outdoor solid-state lighting applications, it provides extended temperature range operation down to -40 °C with guaranteed electrical specification.

The main feature of this IC is a special circuit (Input Current Shaper, ICS), that enables High-PF quasi-resonant flyback converters to draw a theoretically sinusoidal input current from the power line, unlike the traditional control.

In practice, with little effort it is possible to achieve a total distortion of the input current (THD) lower than 10% at full load and lower than 20% at 30% load over the entire input voltage range.

The IC is provided with a control input intended for being driven by the phototransistor of an optocoupler to close a secondary-regulated isolated control loop. However, with the addition of a simple external circuitry it can be used to close a primary-regulated voltage loop as well.

The HVLED007 includes protection features to handle overload, short-circuit and overvoltage conditions.

The totem-pole output stage, capable of 600 mA source and 800 mA sink current, is suitable for big MOSFET drives which, combined with the other features, makes the device an excellent low-cost solution for EN61000-3-2 compliant SMPS up to 100 W.

Table 1. Device summary

Order code	Package	Packaging
HVLED007	SO8	Tube
HVLED007TR		Tape and Reel

Contents

1   Block diagram

Figure 1. Block diagram
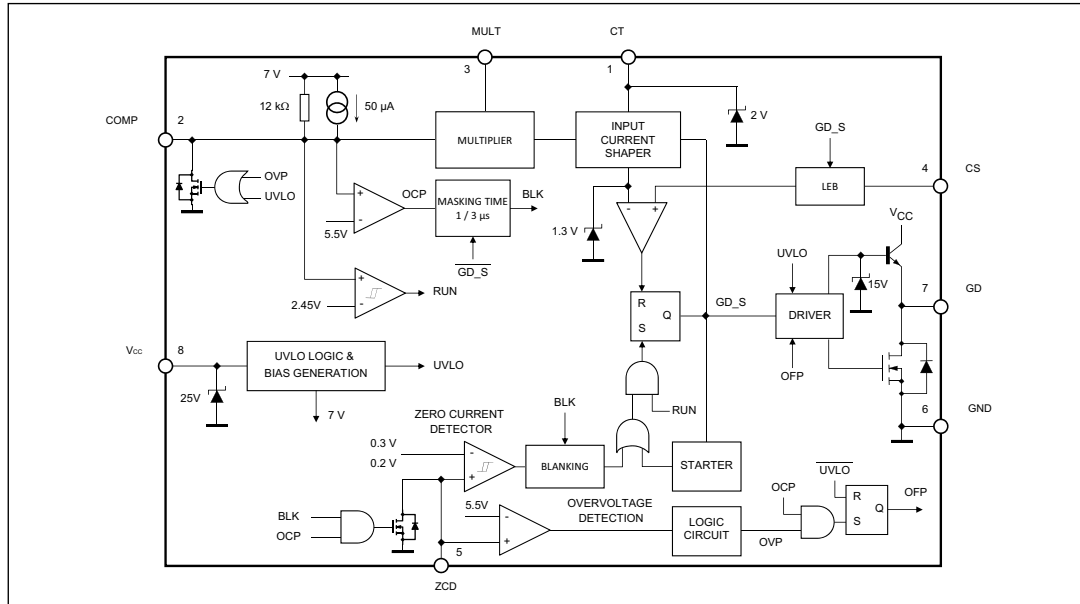
Table 2. Absolute maximum ratings

Symbol	Pin	Parameter	Value	Unit
V_{CC}	8	IC supply voltage (Icc ≤ 20 mA)	-0.3 to VZ[1]	V
I_{GD}	7	Output totem pole peak current	Self-limited	A
V_{CT}	1	Voltage range	-0.3 to $V_{CTsat.hi}$[1]	V
I_{CT}	1	Maximum sink current ($V_{CT} \geq V_{CTsat.hi}$[1])	2.5	mA
V_{COMP}	2	Voltage range	$V_{COMPsat.lo}$[1] to $V_{COMPsat.hi}$[1]	V
$I_{COMP.SOU}$	2	Maximum source current ($V_{COMP} \leq V_{COMPsat.lo}$[1])	2	mA
$I_{COMP.SNK}$	2	Maximum sink current ($V_{COMP} \geq V_{COMPsat.hi}$[1])	0.8	mA
V_{MULT}	3	Voltage range	-0.3 to 8	V
V_{CS}	4	Voltage range	-0.3 to 8	V
V_{ZCD}	5	Voltage range	V_{ZCDL}[1] to 8	V
I_{ZCD}	5	Maximum source current ($V_{ZCD} \leq V_{ZCDL}$[1])	-3	mA
Ptot		Power dissipation @Tamb = 50°	0.65	W
Tj		Junction temperature operating range	-40 to 150	°C
Tstg		Storage temperature	-55 to 150	°C

1. See *Section 3: Electrical characteristics* for parameter definition and value.

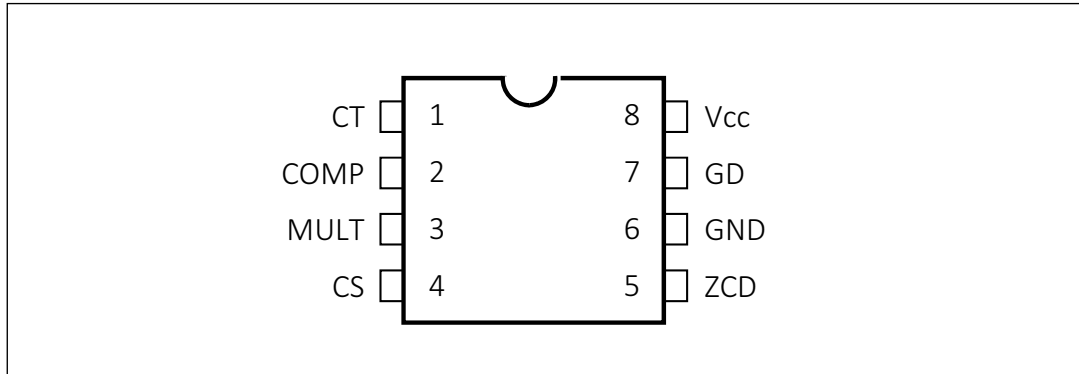# 2   Pin connections

Figure 2. Pin connection (top view)

Table 3. Thermal data

Symbol	Parameter	Value	Unit
Rth j-amb	Max. thermal resistance, junction-to-ambient	150	°C/W

Table 4. Pin functions

N.	Name	Function
1	CT	Input current shaper (ICS) circuit. A capacitor connected from this pin to ground (pin #6) is alternately charged and discharged internally, and the voltage developed across this capacitor is used as the reference for the current loop.
2	COMP	Control input for PWM regulation. The pin is driven by the phototransistor (emitter-grounded) of an optocoupler to modulate its voltage by modulating the current sunk. A capacitor placed between the pin and ground (pin #6), as close to the IC as possible to reduce noise pick-up, is useful to get a clean control voltage. The dynamics of the pin are in the 2.5 to 5.5 V range. A voltage lower than 2.5 V activates burst-mode operation. The voltage at the pin is bottom-clamped at about 2.2 V.
3	MULT	Main input to the multiplier. This pin is connected to the rectified mains voltage via a resistor divider. A capacitor placed between the pin and ground (pin #6), as close to the IC as possible is useful to reduce noise pick-up.
4	CS	Input to the PWM comparator. The current flowing in the MOSFET is sensed through a resistor, the resulting voltage is applied to this pin and compared with the internal reference generated by the ICS circuit, to determine MOSFET's turn-off.
5	ZCD	Transformer demagnetization sensing input for transition-mode (quasi-resonant) operation. A negative-going edge triggers MOSFET's turn-on. A voltage exceeding 5.5 V during MOSFET's OFF-time forces an internal discharge of the COMP pin (#2) below the burst-mode threshold. As a consequence, the IC is temporarily stopped (overvoltage protection). This function is strobed and digitally filtered to increase noise immunity.
6	GND	Ground. Current return for both the signal part of the IC and the gate driver.

Table 4. Pin functions (continued)

N.	Name	Function
7	GD	Gate driver output. The totem pole output stage is able to drive power MOSFETs and IGBTs with a peak current of 600 mA source and 800 mA sink. The high-level voltage of this pin is clamped at about 12 V to avoid excessive gate voltages in case the pin is supplied with a high Vcc.
8	V_{CC}	Supply voltage of both the signal part of the IC and the gate driver. The supply voltage upper limit is extended to 22.5 V min. to provide more headroom for supply voltage changes. Sometimes a small bypass capacitor (0.1 µF typ.) to ground (pin #6) might be useful to get a clean bias voltage for the signal part of the IC.

3 Electrical characteristics

(Tj = -40 to 125°C, Vcc=12, Co = 1 nF; unless otherwise specified.)

Table 5. Electrical characteristics

Symbol	Parameter	Test condition	Min.	Typ.	Max.	Unit
Supply voltage						
V_{CC}	Operating range	After turn-on	10.5	-	22.5	V
V_{CCon}	Turn-on threshold	Positive-going	11.7	12.5	13.3	V
V_{CCoff}	Turn-off threshold	Negative-going	9.5	10	10.5	V
Hys	Hysteresis	-	2.2	-	2.8	V
V_Z	Zener voltage	Icc = 20 mA	22.5	25	28	V
Supply current						
$I_{start-up}$	Start-up current	Before turn-on, Vcc = 11 V	-	30	60	µA
Iq	Quiescent current	After turn-on, V_{MULT} = 1 V, V_{COMP} = $V_{COMPsat.hi}$, V_O = V_{OL}	-	2.5	3.9	mA
		During burst mode	-	1.7	2.5	mA
I_{CC}	Operating supply current	@ 70 kHz, D = 50%, V_{MULT} = 1V, V_{COMP} = $V_{COMPsat.hi}$	-	3.5	5.5	mA
Input current shaper						
V_{CT}	Operating range	-	0	-	1.5	V
$V_{CTsat.hi}$	Upper clamp voltage	[1]	1.5	2	2.5	V
R_T	Internal discharge resistor	-	-	8.3	-	kΩ
V_{CT_OL}	Overload detection threshold	Positive-going[1]	1.25	1.4	1.6	V
PWM control input						
$V_{COMPsat.hi}$	Upper saturation voltage	-	5.8	6.2	6.7	V
V_{COMP_OL}	Overload detection threshold	Positive-going	5.25	5.5	5.7	V
ΔV_{COMP_OL}	Comparator hysteresis	Negative-going	-	100	-	mV
V_{COMPlo}	Lower end of regulation range	[2]	2.35	2.5	2.65	V
V_{COMP_BM}	Burst-mode threshold	Negative-going[2]	2.3	2.45	2.6	V
ΔV_{COMP_BM}	Comparator hysteresis	Positive-going	-	50	-	mV
$V_{COMPsat.lo}$	Lower clamp voltage	ICOMP = -700 µA	2.05	2.2	2.35	V
$I_{COMPsat}$	Source current	V_{COMP} = $V_{COMPsat.hi}$	-	50	-	µA
$I_{COMPmax}$	Maximum source current	V_{COMP} = V_{COMP_BM}	-	350	600	µA

Table 5. Electrical characteristics (continued)

Symbol	Parameter	Test condition		Min.	Typ.	Max.	Unit
R_{COMP}	Equivalent dynamic resistance	$V_{COMPlo} < V_{COMP} < V_{COMP\_OL}$		8	12	19	kΩ
Multiplier input							
I_{MULT}	Input bias current	V_{MULT} = 0 to 4 V		-	-	-1	µA
V_{MULT}	Linear operation range	-		0 to 3	-	-	V
ΔV_{cs}	Output max. slope	V_{MULT} = 0 to V_{csmax}		1	1.1	-	V/V
ΔV_{MULT}		$V_{COMP} = V_{COMPsat.hi}$				-	-
K_M	Gain	V_{MULT} = 1 V, V_{COMP} = 5.25 V		0.375	0.4	0.45	1/V
Current sense comparator							
I_{CS}	Input bias current	V_{CS} = 0 to V_{CSmax}		-	-	-1	µA
$t_{d(H-L)}$	Delay to output	-		-	240	-	ns
t_{LEB}	Leading edge blanking	After turn-on of GD V_{MULT} = 1 V		100	200	300	ns
V_{CSmax}	Current sense reference clamp	$V_{COMP} = V_{COMPsat.hi}$	Tj = 25°C	1.25	1.3	1.35	V
			-	1.2	-	1.4	
Zero current detector							
V_{ZCDA}	Arming voltage	Positive-going edge[3]		0.2	0.3	0.4	V
V_{ZCDT}	Triggering voltage	Negative-going edge[3]		0.15	0.2	0.25	V
V_{ZCDL}	Lower clamp voltage	I_{ZCD} = -50 µA to -2.5 mA		-0.15	0	0.1	V
V_{ZCDmax}	Maximum operating voltage	-		7	-	-	V
I_{ZCDb}	Input bias current	V_{ZCD} = 1 V to V_{ZCDmax} $V_{COMP} < V_{COMPsat.hi}$, $V_{CT} < V_{CT\_OL}$		-	-	1	µA
I_{ZCDsrc}	Source current capability	$V_{ZCD} = V_{ZCDL}$		-	-	2.5	mA
T_{MASK}	Masking time (after turn-off of GD)	$V_{COMP} < V_{COMP\_OL}$		0.6	1	1.5	µs
		V_{COMP} V_{COMP_OL}		1.8	3	4.5	
$R_{DS(on)}$	Grounding switch ON-state resistance	-		-	300	-	Ω
Output overvoltage							
V_{ZCD_OVP}	OVP comparator threshold	Positive-going		5.3	5.5	5.7	V
Starter							
t_{START}	Start Timer period	-		170	280	440	µs
Gate driver							
V_{OL}	Output low voltage	I_{sink} = 100 mA		-	0.6	1.2	V
V_{OH}	Output high voltage	I_{source} = 5 mA		9.5	10.3	-	V
I_{srcpk}	Peak source current	-		-0.6	-	-	A

Table 5. Electrical characteristics (continued)

Symbol	Parameter	Test condition	Min.	Typ.	Max.	Unit
I_{snkpk}	Peak sink current	-	0.8	-	-	A
t_f	Voltage fall time	-	-	30	70	ns
t_r	Voltage rise time	-	-	60	130	ns
V_{Oclamp}	Output clamp voltage	I_{source} = 5mA; Vcc = 20 V	10	12	15	V
-	UVLO saturation	Vcc= 0 to V_{CCon}, I_{sink}= 2 mA	-	-	1.1	V

1. Parameters tracking each other.

2. Parameters tracking each other.

3. Parameters tracking each other.

4 Application information

4.1 Introduction

The HVLED007 is intended to drive Hi-PF QR flyback converters, an extremely popular topology in SSL applications because it is very cost-effective and addressable with the same transition-mode (TM) PFC controllers used for boost PFC stages. However, the TM control technique that in boost PFC stages theoretically provides a sinusoidal input current and unity power factor, in Hi-PF QR flyback converters features inherent distortion of the input current, as depicted in the diagrams of *Figure 3*.

Figure 3. Input current distortion in Hi-PF QR flyback converters with traditional TM control: current shape and resulting total harmonic distortion and power factor vs. Kv (= Vinpk/VR) ratio
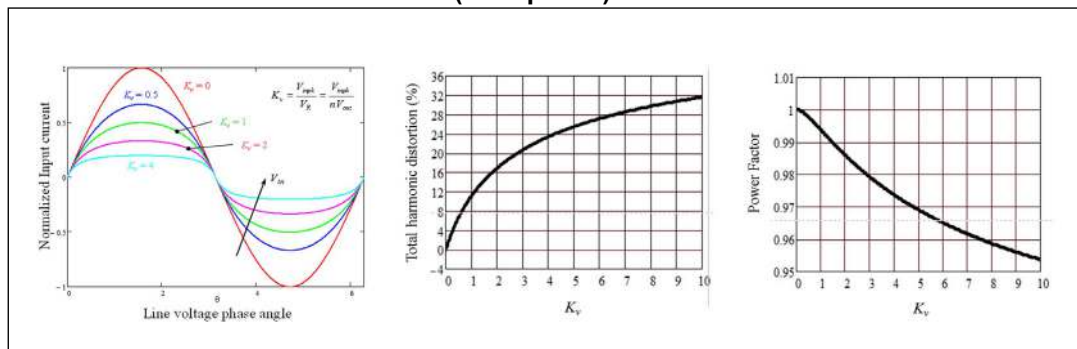
Traditionally, to keep current distortion within acceptable limits, the converter is designed to operate with low K_v (= V_{inpk}/V_R) values, achieved using a large reflected voltage V_R = (N_{pri} / N_{sec}) V_{out}. This, however, requires the use of a power switch (MOSFET) with higher breakdown voltage.

Additionally PFC controllers intended for boost topology, this being a non-isolated topology, do not normally have on-board protection functions suitable for a flyback converter and that therefore need to be implemented with additional external circuits. On the other hand, they have provisions on board that are little useful in an isolated topology like a flyback (e.g. the error amplifier).

The HVLED007 addresses these aspects specifically, providing a novel TM control technique able to provide a sinusoidal input current and unity power factor in flyback converters as well and protection functions typical of offline flyback controller ICs.

4.2 Input current shaping function - operating principle

In a Hi-PF QR flyback converter powered from an AC line with a sinusoidal voltage V_{in} (θ) = V_{inpk} sin θ, (with $\theta = 2\pi f_{line} t$) the input current is the average of the primary current, which flows only during the ON-time of the power switch and is a series of triangles separated by voids corresponding to the OFF-time of the power switch (see current waveforms in *Figure 4*). This can be expressed quantitatively as follows:

Equation 1

$$I_{in}(\theta) = \frac{1}{2} Ip_{pk}(\theta) \frac{T_{ON}}{T(\theta)}$$

Figure 4. Hi-PF QR flyback converter with the traditional TM control: current waveforms
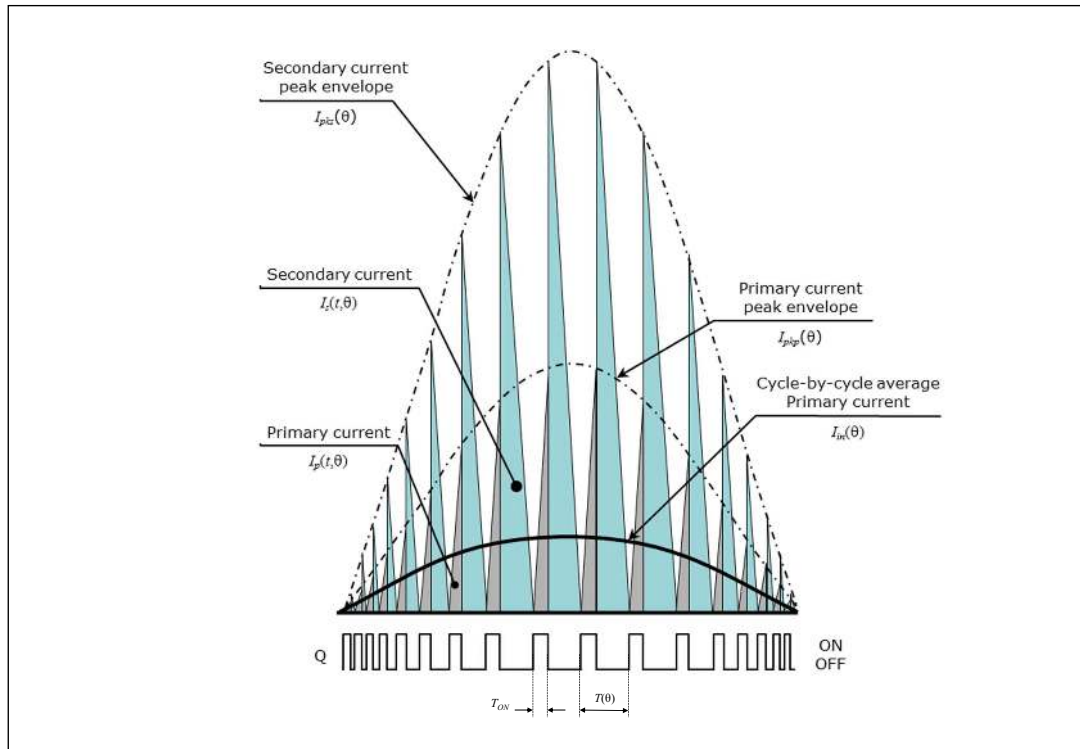
With the traditional TM control method, the term $Ip_{pk}(\theta)$, the peak envelope of the primary current, is sinusoidal ($Ip_{pk}(\theta) = Ip_{pk} \sin \theta$). The distortion stems from the term $T_{ON} / T(\theta)$, due to the primary current being chopped, which is not constant (T_{ON} is constant, $T(\theta)$ is not).

This distortion is prevented if the flyback converter is operated with a fixed switching frequency in the Discontinuous Conduction Mode (DCM). However, there are a few benefits in using TM operation that are lost when operating with a fixed frequency (FF): lower conducted EMI emissions, safer operation under short-circuit conditions, valley-switching or even true soft-switching (zero-voltage switching, ZVS).

The idea behind the novel TM method is to distort the current reference $Vcs_{ref}(\theta)$ that determines $Ip_{pk}(\theta)$ ($Ip_{pk}(\theta) = Vcs_{ref}(\theta) / Rs$) by a term $T(\theta) / T_{ON}$: this cancels out the term $T_{ON} / T(\theta)$ introduced by averaging and results in a sinusoidal average primary current, i.e. in a sinusoidal input current. Then, the control objective can be expressed in the following terms:

Equation 2

$$Vcs_{ref}(\theta) = Vcs_x \sin \theta \frac{T(\theta)}{T_{ON}(\theta)}$$

Note that in *Equation 2* also T_{ON} is denoted as a function of the instantaneous line phase θ; in fact, with the novel method it is no longer constant as in the traditional method.

The "Input Current Shaper" (ICS) that implements this basic idea is shown in *Figure 5* along with the overall control loop inside the IC.

Figure 5. Input current shaper (ICS) block and its interconnection with HVLED007 control
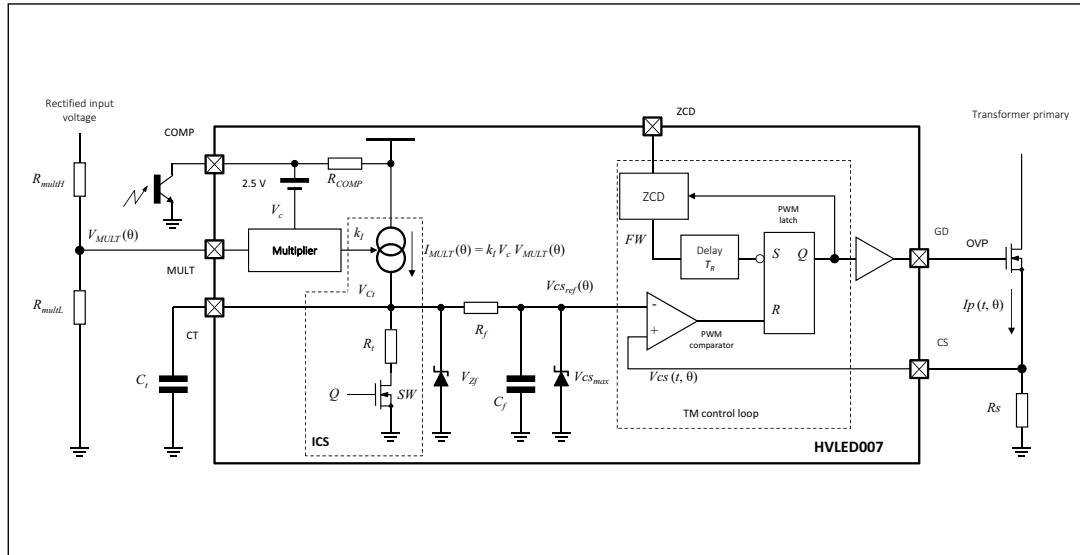
The ON/OFF mechanism of the external power switch is exactly the same as in the traditional TM method: the power switch is turned on as the secondary current zeroes (with a delay T_R to achieve valley switching, see "*Section 4.8: Zero current detection and triggering block (pin ZCD); starter*") and turned off when the voltage Vcs (t, θ) on the current sensing input CS (proportional to the primary current Ip (t, θ)) reaches the reference value Vcs_{ref} (θ). Note that the explicit dependence on time (t) denotes cycle-by-cycle quantities.

The difference between the traditional TM method and that implemented in the HVLED007 is in the way the reference Vcs_{ref} (θ) is generated. In the traditional TM method, Vcs_{ref} (θ) is generated by taking the input voltage as the template and adjusting its amplitude with feedback loop control voltage via the multiplier; in the HVLED007 the output of the multiplier is processed by the ICS circuit highlighted in the dotted box before being provided to the PWM comparator. The ICS circuit is composed of the current generator I_{MULT} (θ), the external capacitor C_t connected between pin CT and ground and a switched resistor R_t that is connected in parallel to C_t during the ON-time T_{ON} (θ) of the power switch through the switch *SW*. The current generator provides the charging current for C_t, given by:

Equation 3

$$I_{MULT} (\theta) = k_I \left[K_p \left(V_{inpk} \, sin\theta \right) V_c \right]$$

where $K_p = R_{multL} / (R_{multH} + R_{multL})$ is the voltage gain of the resistor divider that senses the rectified input voltage. The key waveforms are shown in *Figure 6*.

Assuming $T(\theta) << R_t \, C_t << 1/(2 \, f_{line})$, to a first approximation the voltage ripple across the capacitor C_t can be neglected and the current I_{MULT} (θ) can be considered constant in a switching cycle. The average voltage V_{Ct} (θ) developed across C_t, which shapes the peak primary current Ip_{pk}(θ), is found by charge balance in a switching cycle:

Equation 4

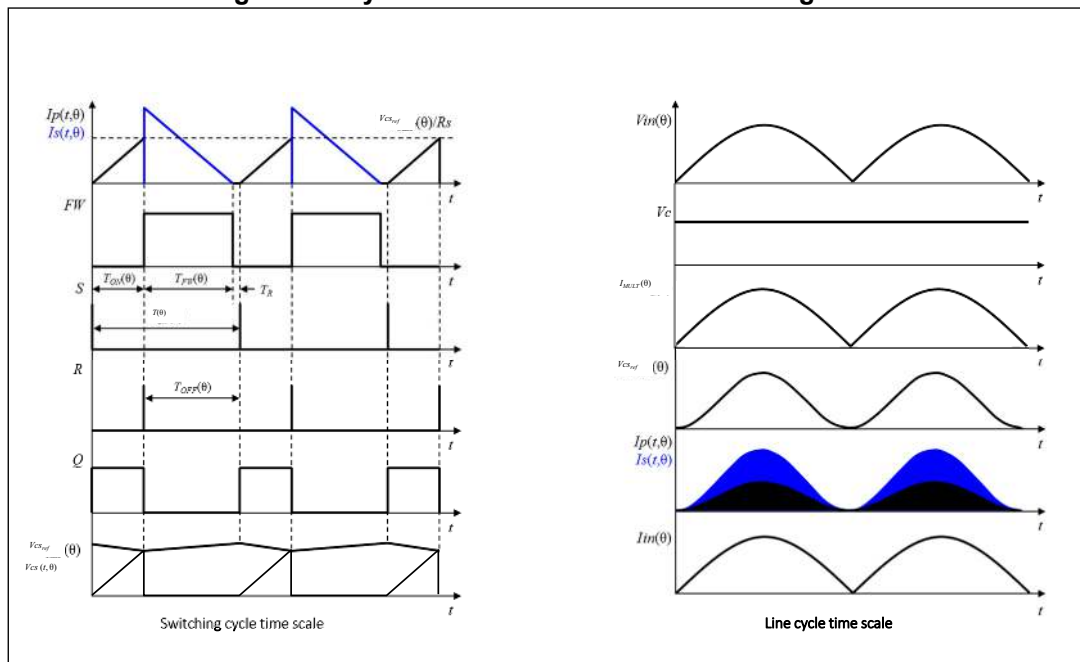$$I_{MULT}\,(\theta)\,T\,(\theta) = \frac{V_{Ct\,(\theta)}}{R_t}\,T_{ON}\,(\theta)$$

Solving (*Equation 4*) for $V_{Ct}\,(\theta)$:

Equation 5

$$V_{Ct}\,(\theta) = I_{MULT}\,(\theta)\,R_t\,\frac{T(\theta)}{T_{ON}(\theta)}$$

Figure 6. Key waveforms of the ICS circuit in figure 5

$V_{Ct}\,(\theta)$ is connected to the (-) input of the PWM comparator through the low-pass filter $R_f\,C_f$, whose purpose is to remove unwanted high frequency noise. The associated time constant ($\approx$ 100 ns) is such that the voltage across C_f is not significantly different from that across C_t, so that $V_{Ct}\,(\theta)$ is actually the reference $Vcs_{ref}\,(\theta)$ for the current loop. If we substitute the expression (*Equation 3*) of I_{MULT} into (*Equation 5*) we find:

Equation 6

$$Vcs_{ref}\,(\theta) = V_{Ct}\,(\theta) = [K_p(V_{inpk}\,sin\,\theta)\,V_c]\;k_I\;R_t\,\frac{T(\theta)}{T_{ON}(\theta)}$$

that has exactly the desired form (*Equation 2*) with:

**Equation 7**

$$Vcs_x = [K_p\,(\,V_{inpk})\,V_c]\,k_I\,R_t$$

In order for (*Equation 6*) to meet the control objective (*Equation 2*) it is necessary that V_c is constant along a line half-cycle. This is a normal design target in any Hi-PF converter, thus the ICS circuit actually meets the control objective. The resulting shape of $Vcs_{ref}(\theta)$ is shown in *Equation 7* for different values of K_v.

It is worth noting that in (*Equation 7*) the parameter K_p is selected by the user (see "*Section 4.12: Suggested step-by-step design procedure of a Hi-PF QR flyback converter based on the HVLED007*"), V_c corresponds to V_{COMP} - 2.5 V and the quantity $k_I R_t$ to the multiplier gain K_M listed among the parameters in "*Section 3: Electrical characteristics*".

The voltage $Vcs_{ref}(\theta)$ is clamped at a value Vcs_{max} that determines the maximum amplitude of the signal on the current sense input CS. This value, listed among the parameters in "*Section 3: Electrical characteristics*", is accurate because it determines the maximum power deliverable by the converter and is used to design the saturation current of the flyback transformer (see "*Section 4.7: Current sensing input (pin CS). Sense resistor (Rs) selection*").

Also the voltage across C_t is internally clamped (at $V_{Zf} > Vcs_{max}$) to prevent a too large dead zone between the external voltage generated across C_t by the shaping circuit and $Vcs_{ref}(\theta)$ internally clamped at Vcs_{max}. For further details about the operating principle and the effect of non-idealities please refer to Reference 1.

Figure 7. Shape of the current reference Vcsref(θ) (5) at different input voltages (i.e. Kv values)
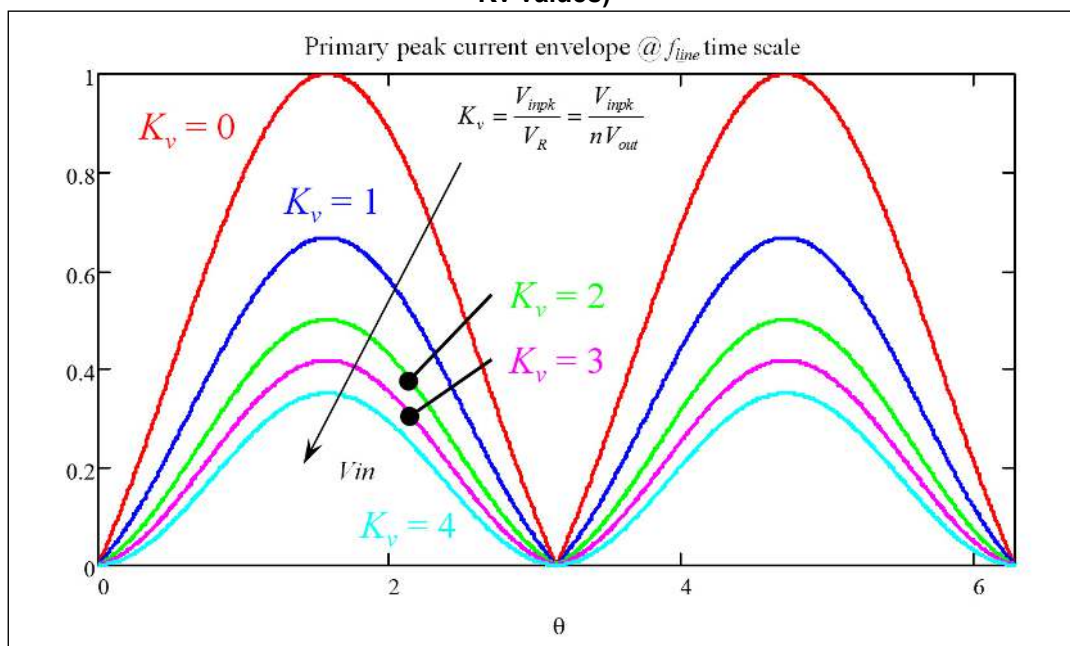
4.3 Operation of a Hi-PF QR flyback converter based on the HVLED007

The ICS circuit changes the profile of the peak current envelope along a line half-cycle (as shown in *Figure 7*) and this slightly changes the timing and the electrical quantities in the converter in steady-state operation as compared to those of a traditionally controlled Hi-PF QR flyback converter [Reference 2]. There are differences in the peak and rms currents but

no difference in the voltage stresses apart from those caused by parasitics and resulting from the different peak currents.

The timing, the control and electrical quantities of a Hi-PF QR flyback converter based on the HVLED007, needed for a proper design, are summarized in *Table 6*, *7* and *8* respectively. The symbolism used has been defined already or is obvious.

Their derivation is based on some simplifying assumptions (in addition to $T(\theta) << R_t C_t << 1/(2 f_{line})$):

- the voltage drop across the EMI filter, the input bridge and the power switch in the ON-state are negligible as compared to the instantaneous line voltage;
- transformer's efficiency is 100% and its windings are perfectly coupled;
- ZCD circuit's delay T_R is negligible, so the converter is assumed to work exactly at the boundary between the continuous and the discontinuous current conduction mode.

Please refer to [Reference 1] for more information on their derivation. It is worth noting that:

- Switching frequency along a line half-cycle is at a minimum on the peak of the sinusoid ($\theta = \pi/2$) and rises along the edges to reach the maximum value at the zero-crossings of the line voltage ($\theta = 0$ and $\theta = \pi/2$).
- The absolute minimum of the switching frequency occurs on the peak of the sinusoid at the maximum input power ($P_{in} = P_{in\_max}$) and at the minimum input voltage ($K_v = K_{v\_min} = V_{inpk\_min} / V_R$).
- The ON-time of the power switch behaves exactly the other way round: it is at a maximum on the peak of the sinusoid, goes to a minimum at the zero-crossings and increases with P_{in}.
- All peak and rms currents have a maximum at the maximum input power ($P_{in} = P_{in\_max}$) and the minimum input voltage ($K_v = K_{v\_min}$).

Table 6. Timing quantities in a HVLED007-based Hi-PF QR flyback converter

Eq. #	Parameter	Expression
1	Power switch ON-time	$T_{ON}(\theta) = 4 \dfrac{Lp}{V_R^2} P_{in} \dfrac{1 + K_v \sin\theta}{K_v^2}$
2	Switching period	$T(\theta) = 4 \dfrac{Lp}{V_R^2} P_{in} \left(\dfrac{1 + K_v \sin\theta}{K_v}\right)^2$
3	Switching frequency	$f_{sw}(\theta) = \dfrac{1}{T(\theta)} = \dfrac{1}{4} \dfrac{V_R^2}{Lp\, P_{in}} \left(\dfrac{K_v}{1 + K_v \sin\theta}\right)^2$
4	Duty cycle	$D(\theta) = \dfrac{T_{ON}(\theta)}{T(\theta)} = \dfrac{1}{1 + K_v \sin\theta}$

Table 7. Control quantities in a HVLED007-based Hi-PF QR flyback converter

Eq. #	Parameter	Expression
1	Control voltage	$V_c = \dfrac{4}{K_v^2 \, V_R^2} \dfrac{P_{in}}{} \dfrac{Rs}{K_m \, K_p}$
2	ICS charge current	$I_{MULT}(\theta) = \dfrac{4}{K_v \, V_R} \dfrac{P_{in}}{} \dfrac{Rs}{R_t} \sin\theta$
3	Current reference	$Vcs_{ref}(\theta) = 4\,Rs\,\dfrac{P_{in}}{V_R}\sin\theta\,\dfrac{1 + K_v\,\sin\theta}{K_v}$
4	Peak-to-peak current reference ripple at switching frequency	$\Delta Vcs_{ref}(\theta) = \dfrac{1}{R_t\,C_t}\left(\dfrac{4P_{in}}{K_v\,V_R}\sin\theta\right)^2\dfrac{Rs\,Lp}{V_R}\,(1 + K_v\,\sin\theta)$

Table 8. Electrical quantities in a HVLED007-based Hi-PF QR flyback converter

Eq. #	Parameter	Expression
1	Peak envelope of primary current	$Ip_{pk}(\theta) = 4\,\dfrac{P_{in}}{V_R}\sin\theta\,\dfrac{1 + K_v\,\sin\theta}{K_v}$
2	Primary peak current	$Ip_{pk} = 4\,\dfrac{P_{in}}{V_R}\,\dfrac{1 + K_v}{K_v}$
3	Primary rms current	$Ip_{rms} = 4\,\dfrac{P_{in}}{V_R}\dfrac{1}{K_v}\sqrt{\dfrac{1}{6} + \dfrac{4}{9\pi}\,K_v}$
4	Primary DC current	$Ip_{dc} = \dfrac{4}{\pi\,K_v}\dfrac{P_{in}}{V_R}$
5	Primary AC current	$Ip_{ac} = 4\,\dfrac{P_{in}}{V_R}\dfrac{1}{K_v}\sqrt{\dfrac{1}{6} - \dfrac{1}{\pi^2} + \dfrac{4}{9\pi}\,K_v}$
6	Secondary peak current	$Is_{pk} = 4\,\dfrac{1 + K_v}{K_v}\,I_{out}$

Eq. #	Parameter	Expression
7	Secondary rms current	$$Is_{rms} = I_{out} \sqrt{2 + \frac{64}{9\pi\, K_v}}$$
8	Secondary DC current	$$Isdc = Iout$$
9	Secondary AC current	$$Is_{ac} = I_{out} \sqrt{1 + \frac{64}{9\pi K_v}}$$
10	Low-frequency secondary current	$$I_o\,(\theta) = 2\,I_{out}\,sin^2\,\theta = I_{out}\,(1 - cos\,2\theta)$$
11	Low-frequency output voltage ripple	$$\Delta V_{o-pk} = I_{out}\frac{1}{2(2\pi f_{line})\,C_{out}} = \frac{I_{out}}{4\pi f_{line}\,C_{out}}$$

As to the dynamic properties of a HVLED007-based Hi-PF QR flyback converter, the ICS circuit is essentially transparent: it only affects the DC gain of the feedback loop. This is intuitive if one recalls that one of the basic assumptions was that the time constant associated to the ICS circuit were << $1/(2\,f_{line})$ and that in Hi-PF converters the crossover frequency of the loop is typically much lower than f_{line}.

Assuming 100% efficiency and that the Hi-PF QR flyback converter powers one or more downstream switching regulators that drive the LED strings, the control-to-output transfer function is:

Equation 8

$$G\,(s)\ =\ \frac{I_{out}}{V_c}\frac{1}{sC_{out}} = \left(\frac{1}{2}\frac{N_{pri}}{N_{sec}}\,K_v\right)^2 K_M\,K_P\frac{V_{out}}{Rs}\,\frac{1}{sC_{out}}$$

4.4   Shaping capacitor (C_t) selection (pin CT)

As previously mentioned, one fundamental assumption for proper operation of the novel control method implemented in the HVLED007 is that the time constant $R_t\,C_t$ associated to the ICS meets the constraints:

Equation 9

$$T(\theta) << R_t\,C_t << 1/(2f_{line})$$

The left-hand side inequality ensures that the voltage across the shaping capacitor C_t is essentially a DC level in any given switching cycle; the right-hand inequality ensures that this DC level is able to change quickly enough to closely follow the ideal reference given by (*Equation 6*) and depicted in *Figure 7*.

With the HVLED007, since R_t is fixed inside the control IC (R_t = 8.3 kΩ) the design objective is to properly select the value of C_t. This is done looking basically at two interrelated factors: the amplitude of the ripple voltage $\Delta V_{Ct}(t, \theta)$ across C_t at the switching frequency and the Total Harmonic Distortion (THD) of the input current. The amplitude of $\Delta V_{Ct}(t, \theta)$ affects also the maximum available signal on the current sense input and, then, the selection of the sense resistor *Rs*. Please refer to "*Section 4.7: Current sensing input (pin CS). Sense resistor (Rs) selection*" for more information concerning this point.

The ripple voltage, generated by the charge and discharge of C_t through $I_{MULT}(\theta)$ and R_t, can be considered essentially triangular and symmetrically superimposed on the slowly varying (at 2 f_{line}) DC value $V_{Ct}(\theta)$. Its peak-to-peak amplitude is given in equation #4 contained in *Table 7*. As discussed in [Reference 1], this ripple causes distortion of the current reference and a reduction of the programmed peak current. Both can be significant if the ripple amplitude is not adequately low.

As a rule of thumb, the maximum peak-to-peak value of $\Delta V_{Ct}(t, \theta)$ should not exceed 10% of the maximum amplitude of $V_{Ct}(\theta)$. Both amplitudes are at a maximum at the maximum input power ($P_{in} = P_{in\_max}$) and minimum input voltage ($K_v = K_{v\_min}$).

Combining equations #3 and #4 of *Table 7*, this condition can be expressed as:

Equation 10

$$\frac{\Delta Vcs_{ref}}{Vcs_{ref}} = \frac{4}{R_t\, C_t} \frac{Lp\, P_{in\_max}}{K_{v\_min}\, V_R^2}\, sin\theta \le 0.1$$

With this choice the programmed peak current $Vcs_{ref}(\theta) - \Delta Vcs_{ref}(\theta)/2$ is less than 5% lower than the value calculated with equations #1 and #2 in *Table 8*, which neglect the contribution of the ripple (see "*Section 4.7: Current sensing input (pin CS). Sense resistor (Rs) selection*" for more details). The distortion caused by the ripple does not exceed 2.5% and the resulting time constant $R_t\, C_t$ is typically in the range of 4 to 5 times the maximum switching period $T(\theta)_{max}$. Experience shows that this value is close to the value that minimizes the THD of the input current for line frequencies in the range of 47 to 63 Hz, which is the range typically specified for applications running from most of the power lines worldwide.

4.5 Control input for isolated feedback and optocoupler driving (pin COMP)

Pin COMP is to be driven by the phototransistor (emitter-grounded) of an optocoupler to modulate its voltage by modulating the current sourced by the pin. *Figure 8* shows the output characteristic of the pin.

Figure 8. Output characteristic of pin COMP and significant levels
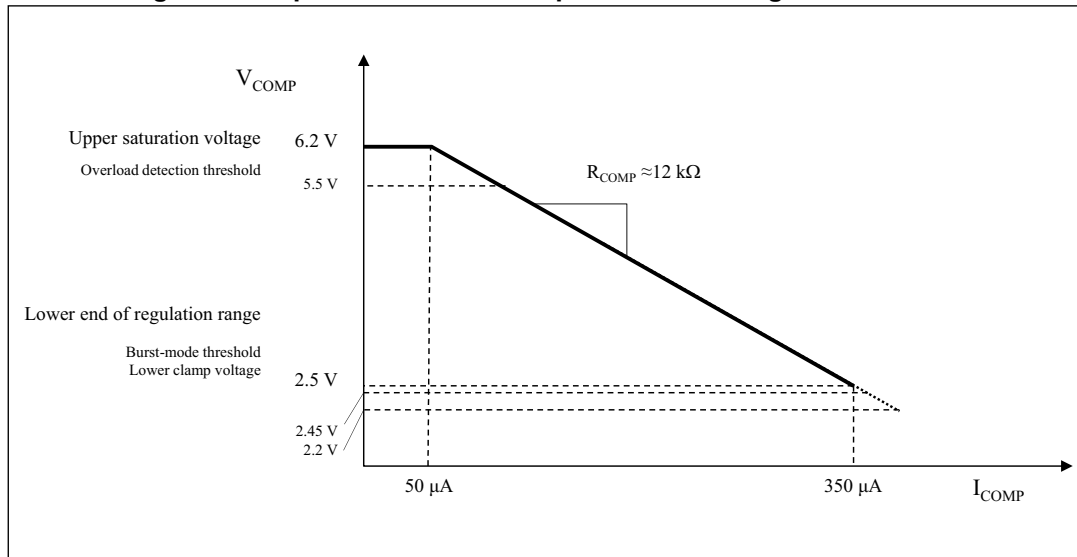
As long as the current I_{COMP} sourced by pin COMP does not exceed 50 µA, the voltage V_{COMP} on pin COMP stays at its upper saturation voltage (6.2 V). For higher I_{COMP} values V_{COMP} falls linearly with a slope corresponding to a resistance R_{COMP} of about 12 kΩ until it reaches the lower end of the regulation range (2.5 V). Values of V_{COMP} higher than 5.5 V are interpreted as an "out of regulation condition" (see "*Section 4.9: Overload and short-circuit protection (OCP function)*"). V_{COMP} is bottom-clamped at 2.2 V to prevent a too large dead-zone under the lower end of the regulation range.

A capacitor placed between the pin and ground, as close to the IC as possible, may be used to either set a pole in the output-to-control transfer function or, in case frequency compensation is done entirely on the secondary side, just reduce noise pick-up. In the latter case it is recommended that the additional pole set in the transfer function by the filter capacitor along with the dynamic resistance of pin COMP (R_{COMP}) is placed at least at a decade above the crossover frequency of the overall open-loop transfer function.

It is worth noting that pin COMP can be driven also by a TS431 to close a control loop in non-isolated applications or in isolated applications with primary sensing regulation. Additionally, forcing pin COMP below 2.45 V by an external switch results in disabling the converter.

- Burst-mode operation. When V_{COMP} falls below V_{COMP_BM} (= 2.45 V) a comparator triggers the so-called "static OVP" function, thus forcing the system to stop and initiating burst-mode operation. While operating in this mode, the HVLED007 provides a series of a few switching cycles spaced out by idle periods where the external power switch is in OFF-state. This ensures system's ability to regulate the output voltage under no load conditions.
  More in detail, the HVLED007 stops switching as V_{COMP} falls below V_{COMP_BM}; the Start Timer (see "*Section 4.8: Zero current detection and triggering block (pin ZCD); starter*") is disabled too. While in the idle state, the converter being stopped, no energy is delivered to the output, so the output voltage starts decaying. The feedback circuit reacts to this droop and, as a consequence, V_{COMP} increases; as it exceeds V_{COMP_BM} by 50 mV, the Start Timer is re-enabled and the IC restarts switching either by a negative-going edge on the ZCD pin (if the idle time is short enough and the drain voltage is still ringing, see "*Section 4.8: Zero current detection and triggering block (pin ZCD); starter*") or by the Start Timer if no edge is detected on the ZCD pin. If the load level has not changed, after

a short while V_{COMP} falls again below V_{COMP_BM} in response to the energy burst and stops again the IC, repeating the same sequence.

With this operating mode the duration of each burst and the idle time are automatically adjusted according to the load conditions: as the load is progressively decreased, the number of switching cycles in each burst becomes smaller and smaller and the duration of the idle time becomes longer and longer. If the load increases, the number of switching cycles in each burst becomes larger and the duration of the idle time becomes shorter, until the operation becomes again continuous.

4.6 Multiplier input for input voltage sensing (pin MULT)

The multiplier input (MULT) is intended to sense the rectified input voltage through a resistor divider to provide a sinusoidal template to the multiplier and the ICS circuit.

The user needs to properly select the voltage gain of the resistor divider K_p. The selection criterion is that K_p needs to be large enough so that the peak of the programming signal $Vcs_{ref}(\theta)$ generated by the ICS circuit at the minimum input voltage can reach the range of the clamp value Vcs_{max} with a level of V_{COMP} voltage lower than the overload detection threshold V_{COMP_OL} (see "*Section 4.5: Control input for isolated feedback and optocoupler driving (pin COMP)*"). The condition to fulfill is:

Equation 11

$$K_p \, V_{inpk-min} = V_{MULTpk\_min} \geq \frac{Vcs_{max\_min}}{K_{M\_min} \, (V_{COMP\_OL\_min} - V_{COMPIo}) \, (1+K_{v\_min})} = \frac{1.231}{1 + K_{v\_min}}$$

with $K_{v\_min} = V_{inpk\_min}/V_R$. It is recommended that K_p be as close to the value given by (*Equation 11*) as possible (compatibly with expected tolerance of K_p), so as to maximize the usage of the regulation range of V_{COMP}

It is also recommended to check that with the selected K_p the amplitude of V_{MULTpk} calculated at the peak of the maximum specified input voltage does not exceed 3 V (linearity limit of the multiplier), in which case the value of K_{v_min} should be increased (i.e. V_R reduced). Normally, this should not happen: the parameters of the ICS circuit have been designed so as to allow a reflected voltage as high as 250 V even in an ultra-wide range application (V_{in} = 85 to 305 Vac).

4.7 Current sensing input (pin CS). Sense resistor (Rs) selection

The PWM comparator (see *Figure 4*) senses the voltage $Vcs(t, \theta)$ across the current sense resistor Rs and, by comparing it to the programming signal $Vcs_{ref}(\theta)$ generated by the ICS circuit, determines the exact time when the external power switch is to be switched off, i.e. $Vcs(T_{ON}(\theta), \theta) = Vcs_{ref}(\theta)$. Its output resets the PWM latch, previously set by the ZCD triggering block (see *Section 4.8: Zero current detection and triggering block (pin ZCD); starter*), which asserts the gate driver output low. The use of PWM latch avoids spurious switching of the external power switch that might result from the noise generated ("double-pulse suppression").

Cycle-by-cycle current limitation is realized by clamping the programming signal $Vcs_{ref}(\theta)$ at a value Vcs_{max} (= 1.3 V typ.). The value of Vcs_{max}, along with that of the sense resistor Rs, determines the overcurrent setpoint, i.e. the maximum peak current $Ip_{pk\,max}$ allowed to flow

on the primary side. If the power demanded by the load requires a larger primary current this results in a no longer regulated output voltage and in a gradual reduction of the power throughput of the converter as the output voltage gets lower.

Figure 9. Effect of ripple on Ct on current sense signal: a) within linear dynamics, close to clamp level; b) signal slightly exceeding clamp level; c) signal exceeding clamp level, with OCP activation
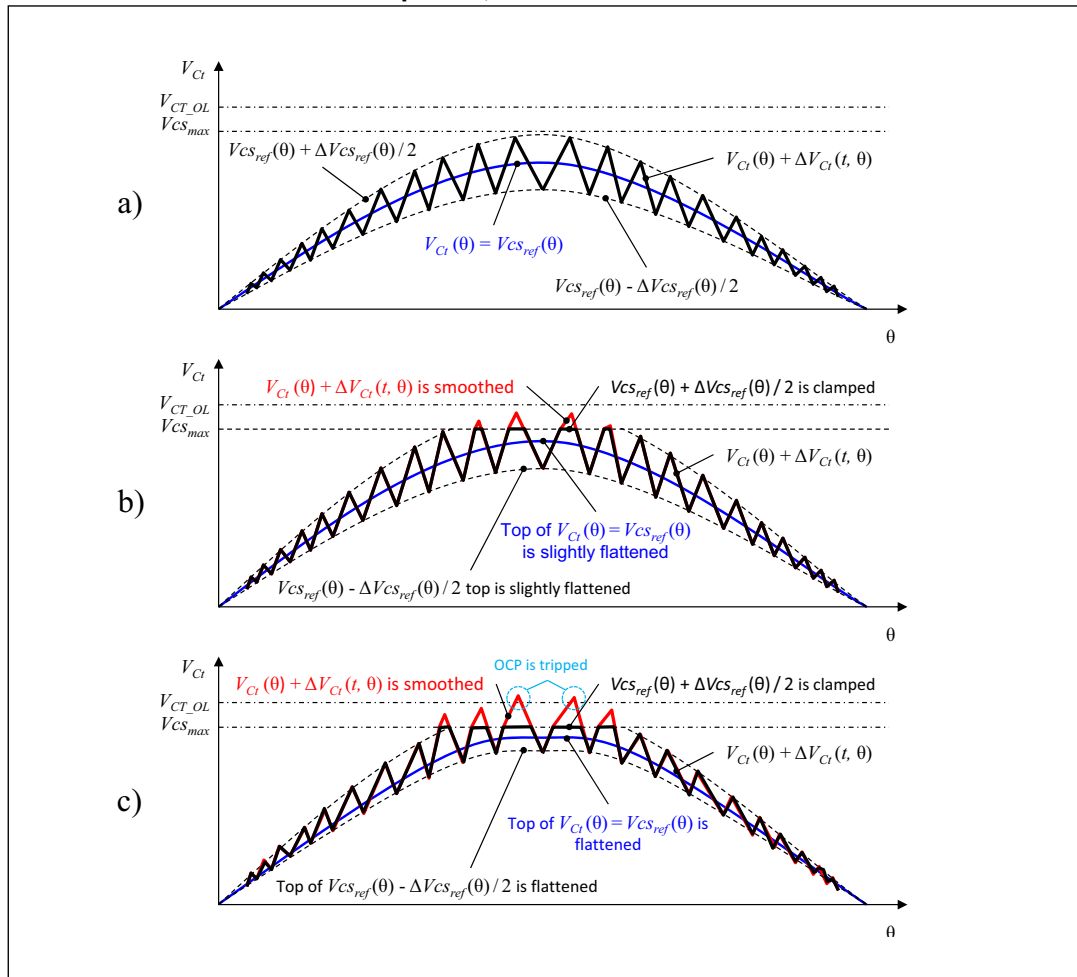
The value of $Ip_{pk\,max}$ is selected so as to ensure with adequate margin that the full load power can be delivered to the output at the minimum specified input voltage, i.e. it is larger than the value provided by equation #2 in *Table 8* with $P_{in} = P_{in\_max}$ and $K_v = K_{v\_min}$.

However, when determining the value of Rs, the effects of the ripple voltage across the shaping capacitor C_t might need taking into account. In fact, as shown in the key waveforms at switching frequency time scale in *Figure 6*, the turn-off of the power switch occurs on the valleys of the ripple. So, the exact turn-off condition is:

Equation 12

$$Vcs\,(T_{ON}(\theta),\theta) = Vcs_{ref}(\theta) - \Delta Vcs_{ref}(\theta)/2$$

and the programmed peak current is actually:

Equation 13

$$Ip_{pk}(\theta) = 4\frac{P_{in}}{V_R} sin\theta \frac{1+K_v sin\theta}{K_v}\left(1-\frac{1}{2R_t C_t}\frac{4Lp P_{in}}{K_v V_R^2} sin\theta\right)$$

which can be derived from equations #3 and #4 in *Table 7*. As previously mentioned, if C_t is selected with the criterion proposed in "*Section 4.4: Shaping capacitor (C_t) selection (pin CT)*", this peak is no more than 5% lower than the value provided by equation #1 in *Table 8*. The control loop easily compensates for that generating a $Vcs_{ref}(\theta)$ only slightly larger than that predicted by equation # 3 in *Table 7* by positioning the control voltage V_{COMP} at a level slightly higher than that predicted by equation #1 in *Table 7*. However there is one more point to be considered and that can be clarified with the aid of *Figure 9*:

* Case a) is that of normal operation just mentioned, i.e. with $Vcs_{ref}(\theta)$ more than $\Delta Vcs_{ref}(\theta) / 2$ away from Vcs_{max} so that the current sense signal is entirely in its linear operation range.

* Case b) occurs when $Vcs_{ref}(\theta)$ is less than $\Delta Vcs_{ref}(\theta) / 2$ away from Vcs_{max}; the peaks of the ripple ($Vcs_{ref}(\theta) + \Delta Vcs_{ref}(\theta) / 2$) is clamped at Vcs_{max}. This impacts indirectly on the envelope of the valleys $Vcs_{ref}(\theta) - \Delta Vcs_{ref}(\theta) / 2$ and, then, on $Ip_{pk}(\theta)$. In fact, as the peaks of the ripple start being clamped, the smoothing resistor R_f has a loading effect on the ICS circuit: the current flowing through R_f to the clamp is stolen from that charging C_t so that the slope of the ascending ramps gets lower, whereas the descending ramps get steeper. This alters the operation of the ICS circuit and results in a $Vcs_{ref}(\theta)$ and an envelope of the valleys that are slightly flattened around the top of the sinusoid. In turn, this flattens the peak of the input current sinusoid, increasing the THD.

* Case c) occurs when the peaks of the ripple ($Vcs_{ref}(\theta) + \Delta Vcs_{ref}(\theta) / 2$) not only exceed Vcs_{max} with all the consequences discussed in the previous case but also the level V_{CT_OL}, which trips the overload protection (see "*Section 4.9: Overload and short-circuit protection (OCP function)*"). This should be the case of a real overload but note that this may occur - normally at low input voltage - even before $Vcs_{ref}(\theta)$ is clamped at Vcs_{max} when $\Delta Vcs_{ref}(\theta)$ is too large (too small C_t and/or too large Rs). This is not the case if C_t is selected with the criterion proposed in "*Section 4.4: Shaping capacitor (C_t) selection (pin CT)*": $\Delta Vcs_{ref}(\theta) / 2$ does not exceed $0.05 \cdot 1.4 = 70$ mV, while the difference $V_{CT\_OL} - Vcs_{max}$ is always greater than 100 mV.

Therefore, as a conclusion, for a given C_t (again, selected as per proposed criterion), if the additional distortion caused at low line by the peaks of the ripple being clamped is acceptable one can consider using the full dynamics of the current sense or nearly so, so that the value of Rs is found from:

Equation 14

$$Rs \le \frac{Vcs_{max\_min}}{Ip_{pk\_max}} = \frac{1.2}{Ip_{pk\_max}}$$

If the additional distortion is to be prevented, the full dynamics needs to be reduced accordingly; then:

Equation 15

$$Rs \leq \frac{Vcs_{max\_min}}{Ip_{pk\_max}} \left(1 - \frac{2}{R_t\,C_t} \frac{Lp\,P_{in\_max}}{K_{v\_min}\,V_R^2} \right) \approx \frac{1.14}{Ip_{pk\_max}}$$

where the last equality holds when C_t is selected as per proposed criterion.

Whatever the design choice is, when designing the flyback transformer make sure that its saturation current I_{sat} meets the condition:

Equation 16

$$I_{sat} \geq \frac{Vcs_{max\_max}}{Rs} = \frac{1.4}{Rs}$$

4.8 Zero current detection and triggering block (pin ZCD); starter

The Zero Current Detection (ZCD) and Triggering blocks switch on the external MOSFET if a negative-going edge falling below 200 mV is applied to the ZCD pin. To do so, the triggering block must be previously armed by a positive-going edge exceeding 300 mV. The voltage at the pin is bottom limited by a clamp that holds the voltage on the pin close to zero during the ON-time of the external power switch.

This arm/trigger operation is typically used to detect transformer demagnetization for TM operation, i.e. close to the boundary between the discontinuous and the continuous conduction mode. An intentional delay T_R is added to the demagnetization detection instant to make the turn-on instant as close as possible to the point where the drain ringing is at a minimum (valley switching).

The signal for the ZCD input is obtained from the transformer's auxiliary winding, typically used also to power the HVLED007. The triggering block is blanked for at least 1 µs after MOSFET's turn-off to prevent any negative-going edge that follows leakage inductance demagnetization from triggering the ZCD circuit erroneously (see "*Section 4.9: Overload and short-circuit protection (OCP function)*").

The interface between the pin and the auxiliary winding is a resistor divider. Its resistance ratio is properly chosen (see "*Section 4.10: Overvoltage protection (OVP function)*") and the upper resistance value R_{zcd} is such that the current sourced by the pin during the ON-time of the power switch is within the rated capability of the internal clamp (2.5 mA):

Equation 17

$$R_{zcd} > 400 \frac{N_{aux}}{N_{pri}}\,V_{inpk\_max}$$

where N_{pri} and N_{aux} are the primary and auxiliary turns number respectively.

At converter power-up, as the IC exits from UVLO, no signal is coming from the ZCD pin, thus an internal oscillator ("Start Timer"), which is active as long as the gate driver (pin GD) is low, sets GD high as its timeout elapses and enables the converter to start up. Switching cycles is initiated by the internal starter until the output voltage and, then, the voltage

developed by the auxiliary winding, becomes high enough to arm the ZCD triggering block and start self-triggered TM operation.

The Start Timer is invoked also whenever the IC stops during burst-mode operation (i.e. as $V_{COMP} < V_{COMP\_BM}$, see "*Section 4.5: Control input for isolated feedback and optocoupler driving (pin COMP)*") or after an overvoltage detection (see "*Section 4.10: Overvoltage protection (OVP function)*") to restart switching activity.

4.9 Overload and short-circuit protection (OCP function)

The purpose of this function is to enable the HVLED007 to effectively control the converter when the load exceeds its maximum specified value or in case of short-circuit at the output so that no component in the power circuit is exposed to risk of failure.

This high-level goal is met by making the converter operate intermittently under these conditions. To allow this, the low-level goal of the OCP function is to make the converter operate at the frequency of the Start Timer, so that the supply voltage of the HVLED007 cannot be kept above the UVLO threshold at all times and the IC continuously shuts down and restarts.

- Detection. Overload and short-circuit conditions (OL-SC) have a twofold detection:
    a) on pin COMP, when its voltage is over the upper end of the regulation range ($V_{COMP} > V_{COMP\_OL}$);
    b) on pin CT, when its voltage V_{Ct} exceeds an internal threshold V_{CT_OL} (= 1.4 V).

OL-SC conditions are then detected by the logic OR of the two detection circuits.

- Corrective actions. The corrective actions aim to prevent the ringing after leakage inductance demagnetization from erroneously triggering a new switching cycle, which would result in high frequency operation under OL-SC conditions.
  Once this has been ensured, one can rely on the natural behavior of TM-operated systems, where the higher the overload, the lower the operating frequency and, therefore the power capability of the converter.
  Eventually, under short-circuit, the output voltage being too low, the ZCD circuit can no longer be armed and the converter works at the frequency of the internal Start Timer (≈3.6 kHz), with an extremely low power capability. Since under these conditions the supply voltage of the IC cannot be kept above its UVLO threshold, the IC continuously shuts down and restarts, as targeted.
  To meet this goal, a time window is generated whenever the external power MOSFET is switched off (signal MSK in the block diagram of *Figure 10*). The synch pulses coming from the ZCD circuit are blanked out during this time window.
  Normally, the duration of this time window is 1 μs but when an OL-SC is detected, it is increased to 3 μs. In addition to blanking the synch pulses coming from the ZCD circuit, during this 3 μs time window the pin ZCD is internally grounded to kill the initial spike that occurs at MOSFET turn-off and prevent the ZCD circuit from being improperly armed.

Figure 10. Functional schematic of the overload and short-circuit protection function
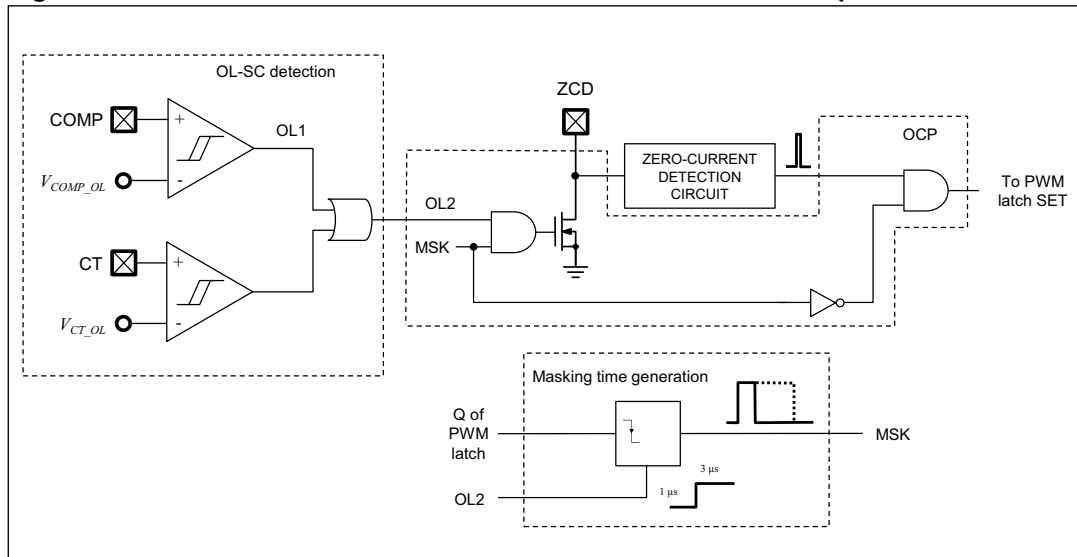
4.10   Overvoltage protection (OVP function)

The purpose of this function is to temporarily stop the operation of the converter in case the output voltage overshoots at start-up or as a result of a sudden load drop, exceeding a preset value.

- Detection. An overvoltage (OV) in the output voltage is sensed through the pin ZCD, which is connected via a resistor divider to the auxiliary winding in the transformer that serves both as zero current detection (to trigger a new switching cycle) and self-supply voltage generator (to power the IC). In fact, during the OFF-time of the external power MOSFET the voltage across the auxiliary winding tracks the output voltage. Tracking is acceptably good for a protection except for a short period after turn-off because strongly affected by the spike caused by the leakage inductance of the transformer and the ringing that follows its demagnetization. To prevent this noise from falsely triggering the OVP function, the detection is done by a comparator referred to a voltage reference V_{ZCD_OVP} (= 5.5 V) on a filtered ZCD signal and the output of this comparator is blanked by the same signal MSK (see *Figure 10*) used in the OCP function.
  If this voltage exceeds V_{ZCD_OVP}, a comparator is triggered and a potential overvoltage condition is assumed. In fact, to reduce sensitivity to noise and distinguish a real failure from a disturbance (e.g. induced during ESD tests), the OVP comparator must be triggered in two consecutive switching cycles in order for the corrective actions to take place.
  More in detail: the first time the OV comparator is triggered a warning flag is set; if in the following switching cycle the OV comparator is triggered again, then the OV condition is confirmed, the corrective action takes place and the warning flag is reset; otherwise no action follows and the warning flag is reset.

- Corrective actions. When an OV condition is detected as specified above, an internal MOSFET switch is turned on, thus connecting a resistor from the pin COMP to GND. The resistor value R_{dis}, which matches R_{COMP} (see *Table 5: Electrical characteristics*), is such that the COMP voltage is definitely taken below the burst-mode threshold. The MOSFET switch is turned off as the COMP voltage falls below the burst-mode threshold.
  The discharge switch is kept in the ON-state also when the IC is in UVLO (provided its

Vcc supply voltage is high enough to define its state) to reset the COMP voltage.
*Figure 11* shows the functional schematic of the OVP circuit.
The OVP detection level V_{outOVP} can be defined by properly selecting the lower resistor R_{ovp} of the divider that connects the pin ZCD to the auxiliary winding according the formula:

Equation 18

$$R_{ovp} = \frac{V_{ZCD\_OVP}}{\dfrac{N_{aux}}{N_{sec}} V_{outOVP} - V_{ZCD\_OVP}} R_{zcd}$$

where N_{sec} and N_{aux} are the secondary and auxiliary turns number respectively. The R_{zcd} value is defined by other application parameters (see "*Section 4.8: Zero current detection and triggering block (pin ZCD); starter*").

Figure 11. Functional schematic of the OVP function
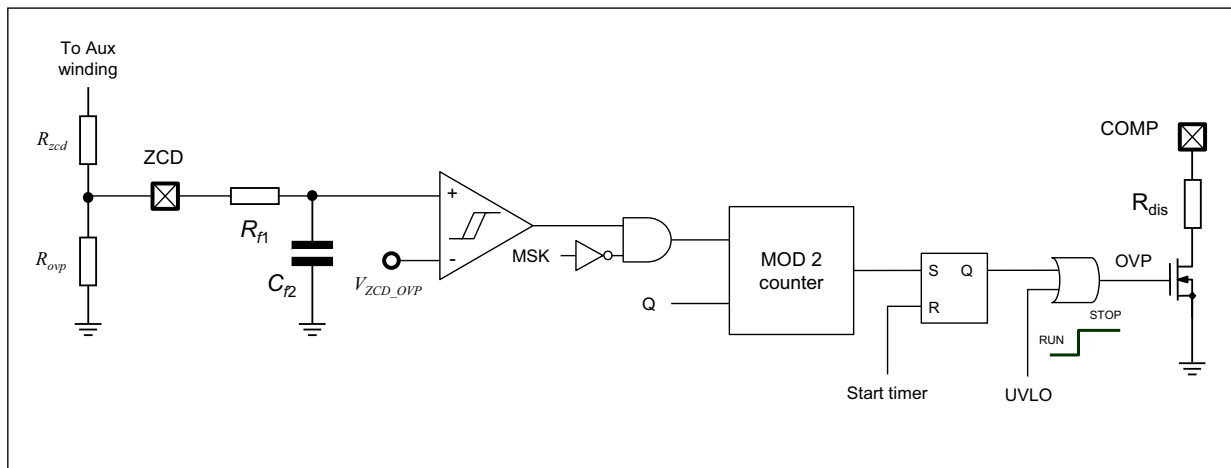
4.11   *Soft-restart function*

This function provides a smooth converter restart limiting the initial primary peak current whenever the IC is temporarily stopped during burst-mode operation (i.e. as V_{COMP} < V_{COMP_BM}, see "*Section 4.5: Control input for isolated feedback and optocoupler driving (pin COMP)*") or after an overvoltage detection (see "*Section 4.10: Overvoltage protection (OVP function)*").

This goal is met by turning on a MOSFET switch connected between pin CT and ground that discharges the external shaping capacitor C_t.

Firstly, the discharge switch is kept in the ON-state as long as the IC is in UVLO (provided its Vcc supply voltage is high enough to define its state) to reset the CT voltage at start-up. Secondly, the discharge switch is turned on as long as the IC is stopped and is turned off when the idle period ends and the gate-drive is turned on. The schematic of *Figure 12* shows the block diagram of the circuit implementing the above-mentioned functionality.

**Figure 12. Functional schematic of the soft restart function**
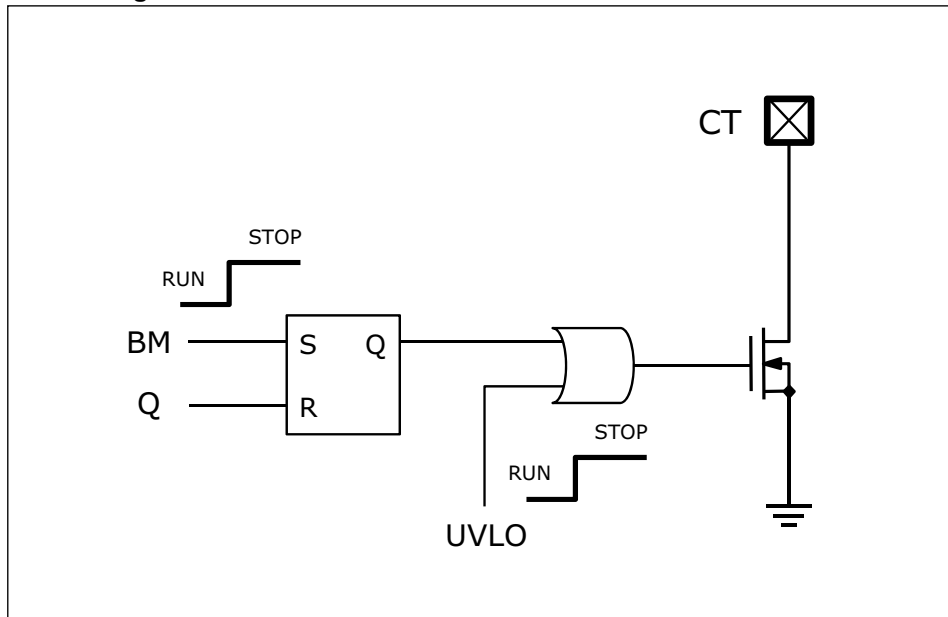
4.12 Suggested step-by-step design procedure of a Hi-PF QR flyback converter based on the HVLED0007

Table 9. Basic electrical specification and key parameters of a Hi-PF QR flyback

Parameter	Symbol
Line voltage range	V_{in_min} - V_{in_max}
Line frequency range	f_{L_min} - f_{L_max}
Regulated output voltage	V_{out}
Output overvoltage level	V_{out_OVP}
Output current range	I_{out_min} - I_{out_max}
Maximum Vout ripple @ 2 fL_min	ΔV_{out_pk-pk}
Expected efficiency at full load (estimated value)	η
Voltage drop on secondary rectifier (estimated value)	V_F
Reflected voltage	V_R
Minimum switching frequency	f_{sw_min}

The proposed design procedure can be outlined in fourteen steps, starting from the design specification detailed in *Table 9* and with reference to the typical application schematic shown in *Figure 13*.

Figure 13. Typical application schematic (reference for suggested design procedure)
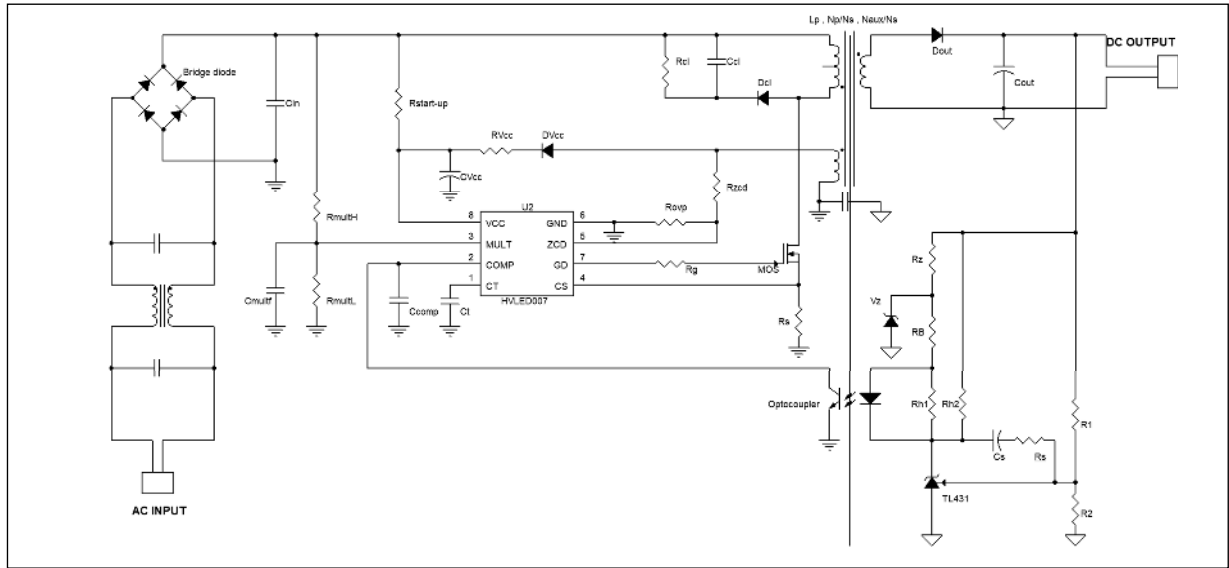
1. Calculate peak voltages corresponding to (V_{in_min} - V_{in_max}) and relevant K_v values (K_{v_min} - K_{v_max}). Calculate estimated maximum input power P_{in_max} from max. load and estimated efficiency:

$$P_{in\_max} = \frac{V_{out} I_{out\_max}}{\eta}$$

2. Calculate operating conditions at V_{in} = V_{in_min} and P_{in} = P_{in_max} with the aid of the equations in *Table 8*, using previously calculated values of $\overline{K}_{v\_min}$ and P_{in_max}.

3. Calculate transformer's primary-to-secondary turns ratio, based on the desired V_R:

$$n = \frac{N_{pri}}{N_{sec}} = \frac{V_R}{V_{out} + V_F}$$

4. Calculate required primary inductance from equation #3 in *Table 6* solved for L_p and with sin θ = 1, K_v = K_{v_min} and P_{in} = P_{in_max}:

$$Lp = \frac{1}{4} \frac{V_R^2}{f_{sw\_min} P_{in\_max}} \left(\frac{K_{v\_min}}{1+K_{v\_min}}\right)^2$$

5. Calculate first-cut value of shaping capacitor from (*Equation 10*) with *sin* θ = 1. This value might be subject to post-design changes to optimize THD of input current or adjust maximum deliverable power.

6. Pick maximum primary peak current I_{ppk_max}; select sense resistor *Rs* using either (*Equation 14*) or (*Equation 15*) and calculate required transformer saturation current I_{sat} from (*Equation 16*).

7. Design transformer with any commonly used procedure using data calculated in steps 2 to 6.

8. Calculate worst-case voltage stress on power switch and secondary rectifier from spec data and actual primary-to-secondary turns ratio.

9. Select primary MOSFET and secondary rectifier using information on their current and voltage stress derived in steps 3 and 7.

10. Use either output voltage ripple or AC current rating, whichever gives the higher capacitance value, to select output capacitor C_{out}.

11. Calculate resistor divider connected to ZCD pin of HVLED007: determine R_{zcd} from (*Equation 17*), then calculate R_{ovp} with (*Equation 18*).

12. Determine multiplier bias gain Kp; pick a value larger than the minimum provided by (*Equation 11*).:

$$Kp \geq \frac{1.231}{V_{inpk\_min} (1+K_{v\_min})}$$

check that the resulting amplitude of V_{MULTpk} at V_{in} = V_{in_max} does not exceed 3 V; if it does, K_{v_min} needs increasing (i.e. V_R needs lowering) and design should restart from step 1.

Individual values of R_{multH} and R_{multL} may be selected based on power consumption considerations.

13. Design clamp circuit that limits leakage inductance spikes with any commonly used procedure with data calculated in step 2.

14. Design feedback circuit and its frequency compensation according to relevant specifications (not included in *Table 9* for simplicity).

5   Referenced documents

1. C. Adragna, G. Gritti, "High-power-factor quasi-resonant flyback converters draw sinusoidal input current", Applied Power Electronics Conference and Exposition, 2015. APEC '15, Conference Proceedings 2015, pp. 498-505, March 2015

2. Design Equations of High-Power-Factor Flyback Converters based on the L6561. Application note AN1059

6 Package information

In order to meet environmental requirements, ST offers these devices in different grades of ECOPACK® packages, depending on their level of environmental compliance. ECOPACK specifications, grade definitions and product status are available at: www.st.com.

ECOPACK is an ST trademark.

Table 10. SO-8 mechanical data

Dim.	mm.			inch		
	Min.	Typ.	Max.	Min.	Typ.	Max.
A	1.35		1.75	0.053		0.069
A1	0.10		0.25	0.004		0.010
A2	1.10		1.65	0.043		0.065
B	0.33		0.51	0.013		0.020
C	0.19		0.25	0.007		0.010
D [1]	4.80		5.00	0.189		0.197
E	3.80		4.00	0.15		0.157
e		1.27			0.050	
H	5.80		6.20	0.228		0.244
h	0.25		0.50	0.010		0.020
L	0.40		1.27	0.016		0.050
k	0° (min.), 8° (max.)					
ddd			0.10			0.004

1. Dimensions D does not include mold flash, protrusions or gate burrs. Mold flash, protrusions or gate burrs shall not exceed 0.15mm (.006inch) in total (both side).

Figure 14. Package dimensions
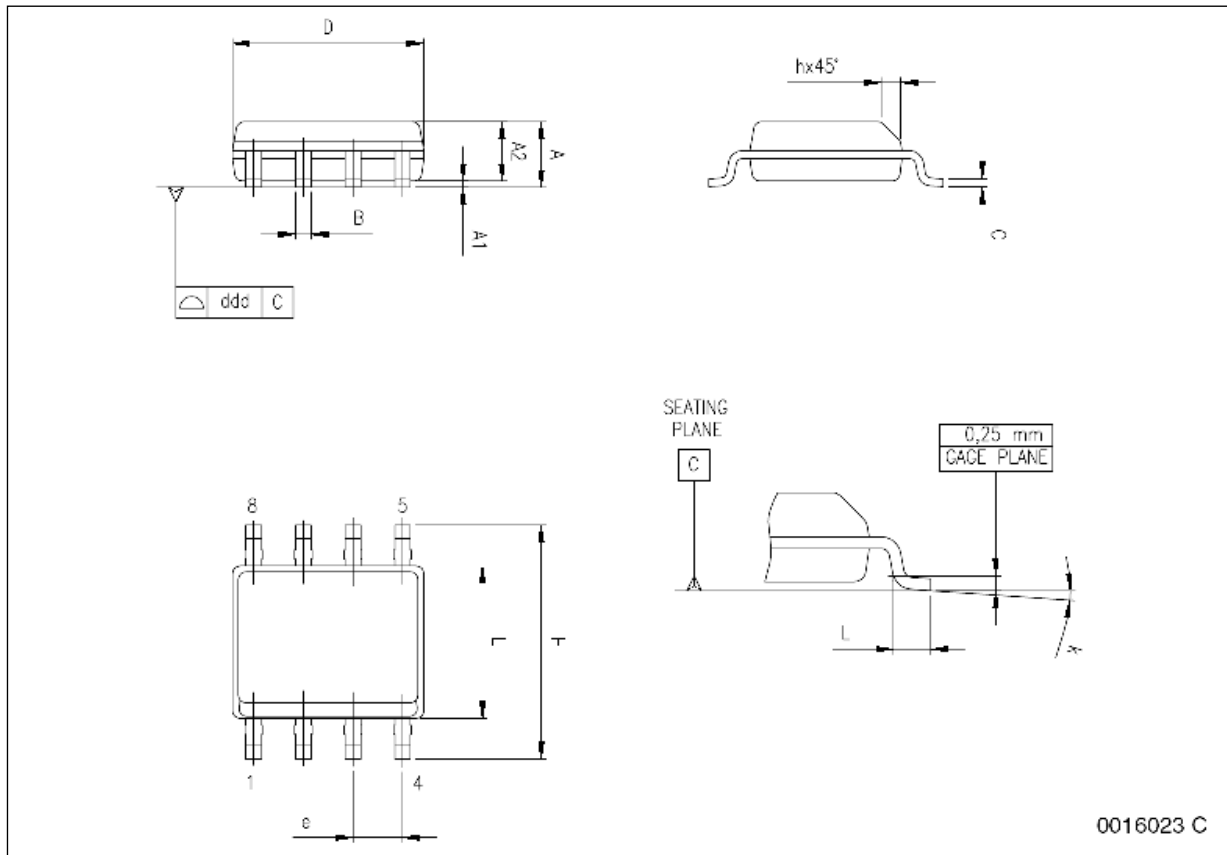
7 Revision history

Table 11. Document history

Date	Revision	Changes
18-Jan-2019	1	Initial version.

IMPORTANT NOTICE – PLEASE READ CAREFULLY